Boletim da Sociedade Astronômica Brasileira, **35**, no. 1, 123-126

Estimating stellar and nebular properties with AlStar in S-PLUS galaxies

J. Thainá-Batista, R. Cid Fernandes, & the S-PLUS team

[1] Universidade Federal de Santa Catarina, Florianópolis, SC, Brazil
e-mail: jullia.thainna@gmail.com, cid@astro.ufsc.br

Abstract. The aim is to study galaxies in our local Universe, observed by the Southern Photometric Local Universe Survey (S-PLUS). Therefore, this first stage of the doctorate was dedicated to the search, use, and improvement of methods that are reliable in obtaining astrophysical properties for S-PLUS galaxies. Several tests were carried out using ALstar, a spectral synthesis code, so that we obtained a new approach to the method, based on an empirical prior, aiming to obtain values with greater accuracy for the emission lines. In this methodology, the properties of stellar populations and emission lines are estimated simultaneously. To test the reliability of the results obtained with ALstar using S-PLUS's 12-band photometry, we ran simulations comparing galaxy property results from a spectral fitting analysis (*input*) from the Sloan Digital Sky Survey (SDSS) with the results of synthetic photometry (*output*) of the S-PLUS perturbed with realistic noise. For a signal-to-noise ratio equal to 50 in the r band, an agreement (*output* − *input*) lower than 0.2 dex, and ±0.2 mag to extinction. For emission line properties, the results were even better, with an agreement within 0.05–0.2 dex for equivalent line widths [O II], Hβ, [O III], Hα, [N II] and [S II]. Good results were also obtained for line ratios, log[N II]/Hα, log[O III]/Hβ, log Hα/Hβ and log[O III]/[O II] with dispersions within 0.09 dex for when the lines involved have equivalent width W > 5 Å. These results are due to the construction of the ALstarnebular base, whose sample space is limited according to the Baldwin–Phillips–Telervich (BPT) diagnostic diagram, and also to the fact that we use $W_{H\alpha+[N\,II]}$ to constrain which side of the BPT the galaxy should be on, considering redshifts at which the Hα and [N II] lines are within the J0660 narrow filter.

[-4pt] **Resumo.** Objetiva-se estudar galáxias do nosso Universo local, observadas pelo Southern Photometric Local Universe Survey (S-PLUS). Dessa forma, essa primeira etapa do doutorado foi dedicada a busca, utilização e aprimoramento de métodos que sejam confiáveis na obtenção de propriedades astrofísicas para galáxias do S-PLUS. Foram feitos diversos testes utilizando o ALstar, código de síntese espectral, tal que obtivemos uma nova abordagem para o método, baseado de um priori empírico, objetivando-se obter valores com maior acurácia para as linhas de emissão. Nessa metodologia, as propriedades de populações estelares e de linhas de emissão são estimadas simultaneamente. Para testar a confiabilidade dos resultados obtidos com o ALstar usando a fotometria de 12 bandas do S-PLUS, fizemos simulações, comparando os resultados de propriedade de galáxias provindos de uma análise de ajuste espectral (*input*) do Sloan Digital Sky Survey (SDSS) com os resultados da fotometria sintética (*output*) do S-PLUS perturbada com ruído realista. Para uma razão sinal-ruído igual a 50 na banda r, obteve-se para as propriedades estelares, massas, idades médias e metalicidades, uma concordância (*output* − *input*) menor que 0.2 dex, e ±0.2 mag para a extinção. Para as propriedades de linhas de emissão, os resultados foram ainda melhores, com uma concordância dentro de 0.05–0.2 dex para larguras equivalentes das linhas [O II], Hβ, [O III], Hα, [N II] e [S II]. Também obteve-se bons resultados para razões de linhas, log[N II]/Hα, log[O III]/Hβ, log Hα/Hβ e log[O III]/[O II] com dispersões dentro de 0.09 dex quando as linhas envolvidas possuem largura equivalente W > 5 Å. Esses resultados se devem a construção da base nebular do ALstar, cujo espaço amostral se limita de acordo com o diagrama de diagnóstico Baldwin–Phillips–Telervich (BPT), e também ao fato de utilizarmos a $W_{H\alpha+[N\,II]}$ para restringir em qual lado do BPT a galáxia deve estar, considerando redshifts nos quais as linhas Hα e [N II] estejam dentro do filtro estreito J0660.

Keywords. galaxies: general – methods: data analysis – techniques: photometric – galaxies: stellar content – astronomical data bases: miscellaneous

1. Introduction

The data used in this work is from the survey The Southern Photometric Local Universe Survey (S-PLUS), which is a project based on an 80 cm robotic telescope, consisting of images on five broad and seven narrow bands spanning the ~ 3500–9000 Å range. More details of S-PLUS can be found in Mendes de Oliveira et al. 2019. This work aims to understand how reliable the stellar populations and emission lines properties of galaxies from S-PLUS are. The follow-up sections are a summary of the complete and detailed work, presented in Thainá-Batista et al. 2023.

2. Method

Our analysis of the galaxies is made through SED fitting, using ALstar, a code of spectral synthesis that performs an algebraic decomposition of an observed spectrum in terms of a spectral base. It uses a stellar population base (an updated version of the Bruzual & Charlot 2003 models) which has 16 ages (t = 1 Myr to 14 Gyr) and 5 metallicities (Z = 0.005 to 3.5$Z_\odot$) and, also (optionally) a emission line base which is composed by 94 components (see Fig.1) that contain the lines: [O II]$\lambda\lambda$3726, 3729 doublet, [O III]$\lambda\lambda$4959, 5007, [N II]$\lambda\lambda$6548, 6584, [S II]$\lambda\lambda$6717, 6731, and the Balmer series (from Hα to Hϵ). A Chabrier 2003 initial mass function is adopted. Dust attenuation is parameterised by the V-band optical depth (τ) and is modelled with a Calzetti et al. (2000) law.

Our method has a new approach to the emission line (EL) base. The components of the EL base are constructed from the BPT diagram and are shown in Fig. 1. Each component has 5 line groups: [O II], Hβ, [O III], Hα, [N II] and [S II].

3. Results

We have 3 different kinds of results. The first one was obtained through simulations, which gave us more control and allowed us to compare all the properties derived from ALstar. The other

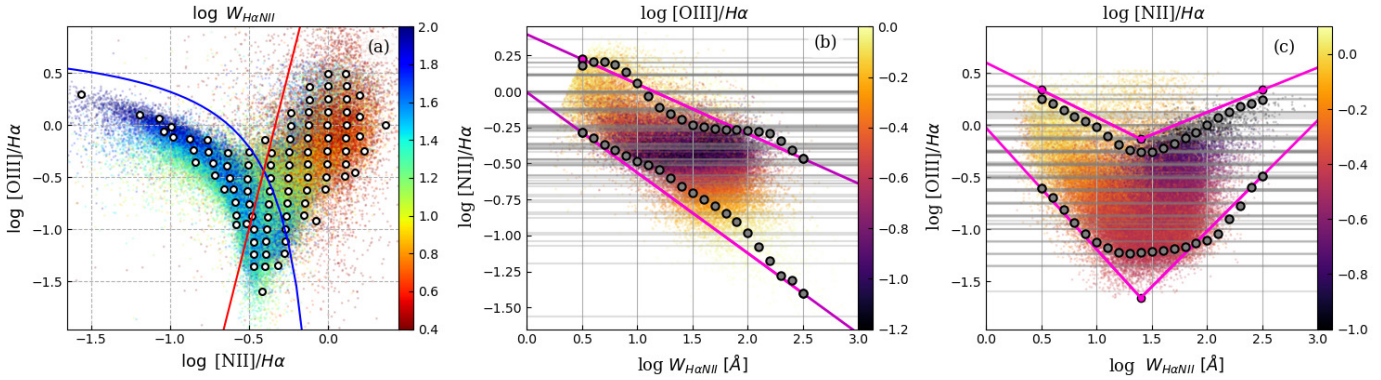

Figure 1. (a) BPTα for SDSS galaxies, dots colored by the log of $W_{H\alpha NII} = W_{H\alpha} + W_{[N\,II]6548} + W_{[N\,II]6584}$ [Å] and our EL base component (white circles). The blue and red curves are part of the EL base restriction scheme. (b) log[N II]/Hα versus $W_{H\alpha NII}$. (c) Like panel b, but for [O III]/Hβ. Dark circles in panels b and c track the 5 and 95 percentile curves, while horizontal gray lines mark the log-line-ratios in the full EL base. The magenta lines show the lower and upper limits imposed to limit the EL base for a given $W_{H\alpha NII}$. These limits refine the left/right wing constraints shown in panel a. Together, they work as a prior which helps estimate EL properties out of the always reliable estimate of $W_{H\alpha NII}$.

two are results from S-PLUS real data, integrated data, and data cube. We have done comparisons for both.

3.1. Simulations

In order to test ALSTAR in the S-PLUS regime we have selected 10473 SDSS galaxies out of those previously analyzed employing full spectral synthesis and detailed EL fitting by (Werle et al. 2019, hereafter W19) with the STARLIGHT and DOBBY. The test consists of computing the synthetic photometry of these galaxies, adding noise, running it through ALSTAR, and comparing its output with that obtained by W19. See Fig. 2, 3 and 4.

Our main intended applications are for galaxies of z low enough so that [N II]6584 is still within the J0660 filter, which corresponds to $z < 0.018$, so all spectra are shifted to $z = 0.01$. Each galaxy is fitted $n_{MC} = 100$ times, perturbing the input photometry with gaussian noise with amplitude defined by the error spectrum ϵ_λ scaled to reach the target SN_r (here, $SN_r = 50$). The error spectrum is derived from statistics of thousands of galaxies observed by S-PLUS.

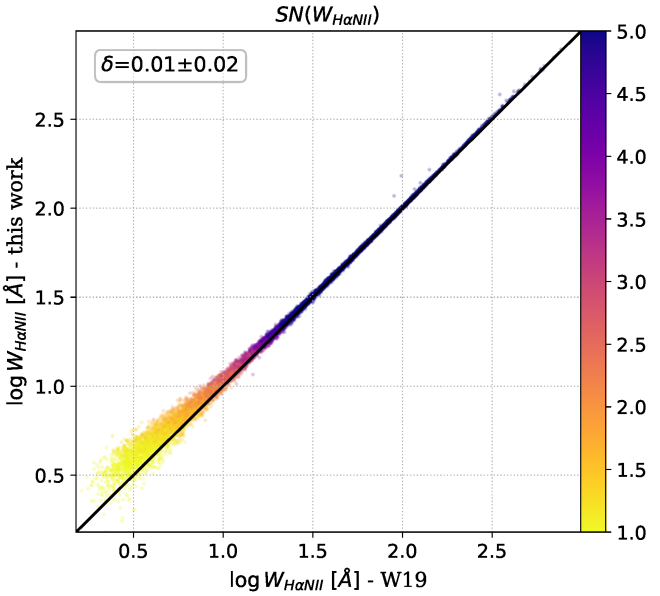

Figure 2. Comparison of the input (SDSS + STARLIGHT + DOBBY) and output (S-PLUS + ALSTAR) values of $W_{H\alpha NII}$. Points are coloured by the ALSTAR-based estimate of the S/N of the combined Hα and [N II]6548, 6584 equivalent widths.

3.2. Applications

3.2.1. Integrated data

We have chosen NGC 1379 (an elliptical galaxy) and NGC 1365 (a barred-spiral), both in the Fornax cluster, to illustrate the application of ALSTAR to integrated light S-PLUS data. The model matches the data to within 1.7% (NGC 1379) and 2.8% (NGC 1365), see Fig. 5. Our fits yield $\log M_\star/M_\odot = 10.48$ and 10.86, for NGC 1379 and NGC 1365, respectively, which agree within ~ 0.06 dex with that obtained by Iodice et al. (2019a) and Raj et al. (2019) on the basis of VST photometry and the Taylor et al. (2011) recipe for M/L_i as a function of $g - i$.

About the stellar populations for NGC 1379, our fits indicate for the whole-galaxy a log of the mean age of $\langle \log t \rangle_L = 10.01$ and $\langle \log t \rangle_M = 10.09$ yr, while Iodice et al. (2019b) obtain similar log age/yr of 10.11 over the central $0.5R_e$ using a different method and data (MUSE-based). Regarding metallicities, our whole-galaxy estimates are $\langle \log Z/Z_\odot \rangle_L = -0.12$ and $\langle \log Z/Z_\odot \rangle_M = -0.17$, while Iodice et al. (2019b) obtain -0.13 over the central $0.5R_e$. For the galaxy NGC 1365 we have also explored a spatially resolved work, see the next section.

3.2.2. Datacube

We have applied the method also in a datacube, given that this is our goal, analyses of spatially resolved galaxies in the local universe, which is where we have more reliable results for the EL properties.

The Fig. 6 shows the principal property maps for the galaxy NGC 1365, and the Fig. 7 shows RGB composites exploring the relations between the properties maps.

To have a complete analysis, we have compared it with the MUSE data. A zoom of the properties with the same colorbar values is shown in Fig. 8.

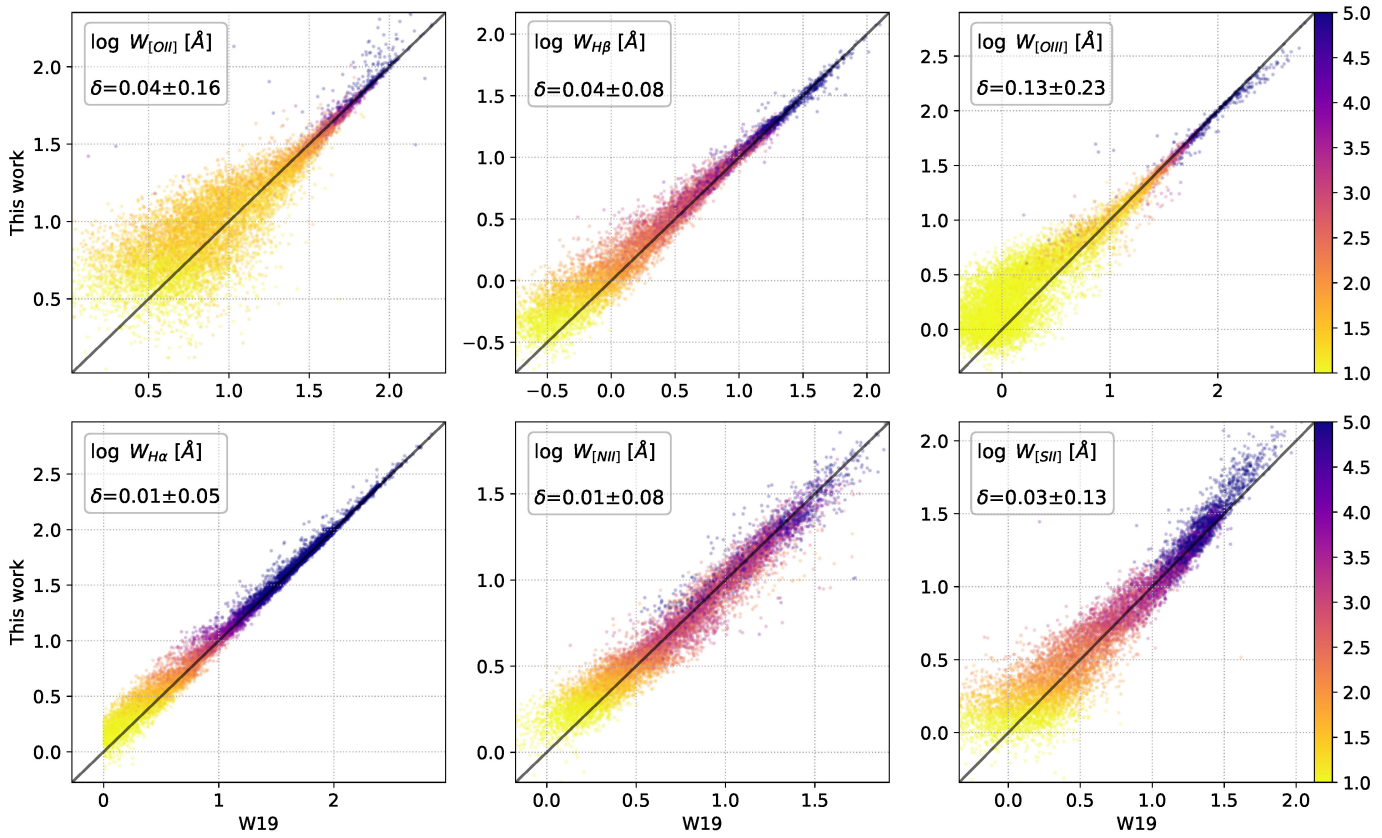

Figure 3. As in Fig. 2, but for W of the individual lines. The colour scale reflects the S/N of the corresponding line.

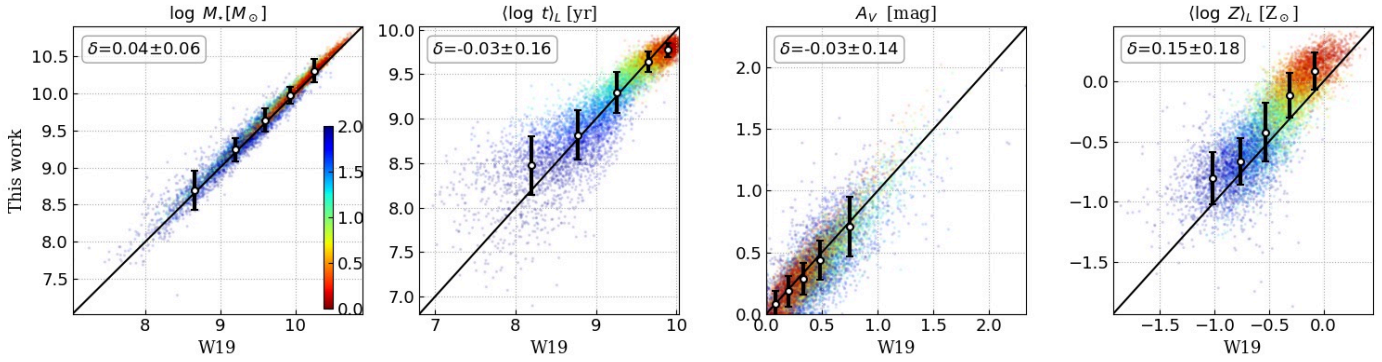

Figure 4. Same comparison of Fig.1(d) but for the stellar properties. Points are colour-coded according to the input value of log $W_{H\alpha}$. Error bars illustrate the (median σ_{NMAD}) dispersion between output and input values for bins along the x-axis.

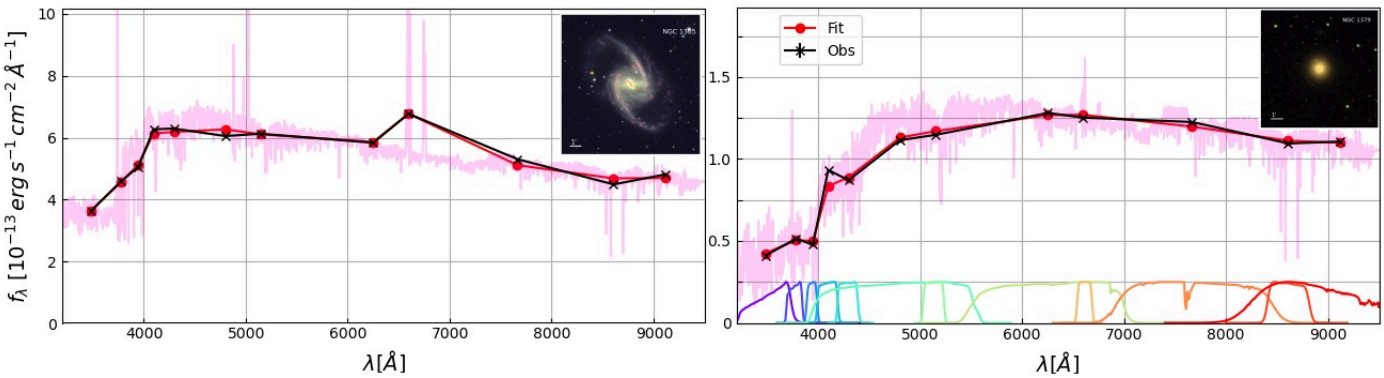

Figure 5. Example AlStar fits of S-PLUS data for two galaxies. The data is plotted in black crosses, while the model photometric fluxes are plotted as red circles. The model spectrum is plotted in magenta.

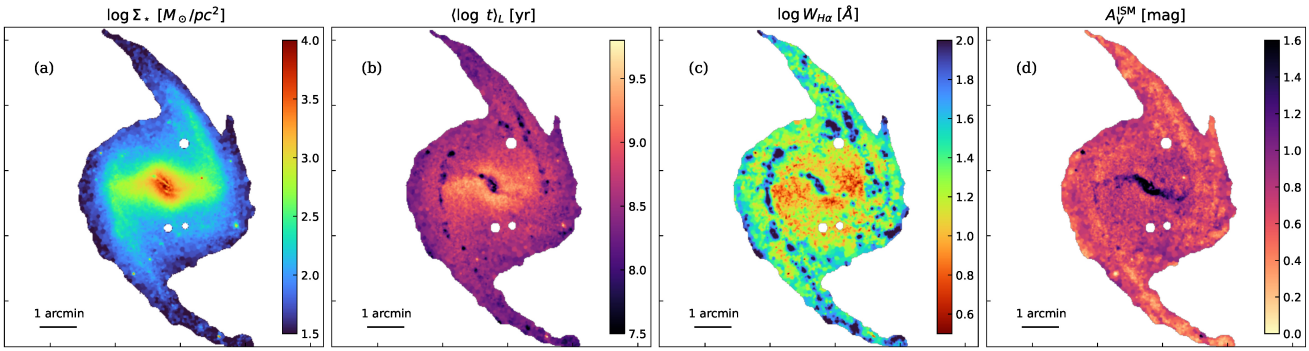

Figure 6. Example of IFS-like science with S-PLUS data for NGC 1365. (a) Stellar mass surface density ($\Sigma_\star$), (b) luminosity weighted mean log age ($\langle \log t \rangle_L$), (c) Hα equivalent width ($W_{\rm H\alpha}$), and (d) stellar extinction (A_V) maps.

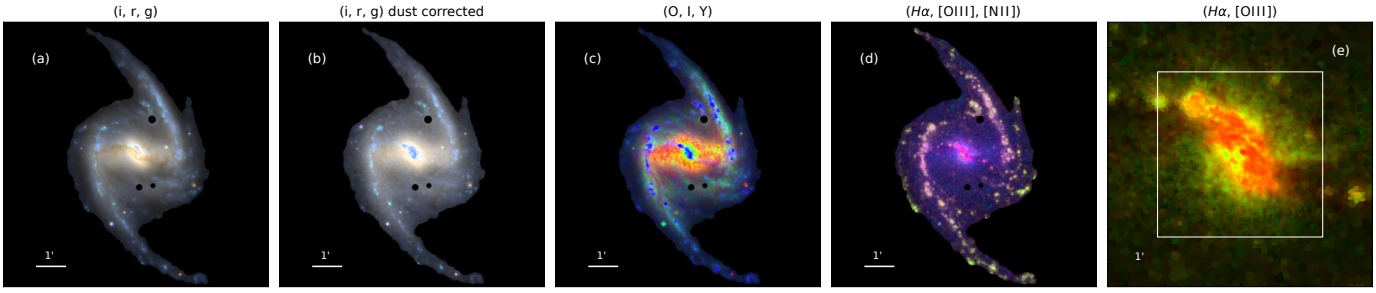

Figure 7. RGB composites combining respectively the (a) observed i, r, and g band fluxes, (b) the dust-corrected i, r, g fluxes, (c) the 5635 Å continuum fluxes associated with old, intermediate, and young populations, (d) the Hα, [O III], and [N II] fluxes. Panel (e) shows a map of Hα (in R) and [O III] (G) of the central region, to be compared to the same map produced by Venturi et al. (2018) (their figure 1) on the basis of MUSE data (field of view shown as a box).

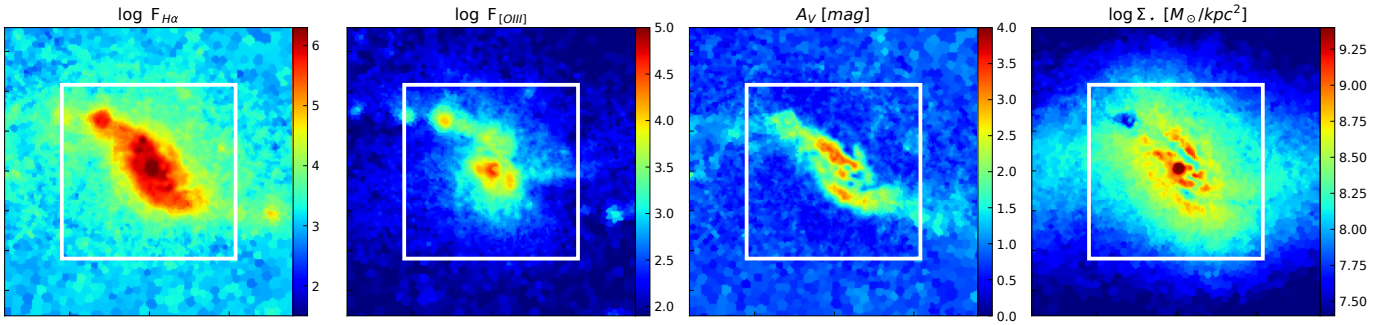

Figure 8. Zoom on the inner maps of $F_{\rm H\alpha}$, $F_{\rm [O\,III]}$ (both in units of 10^{-20}erg s^{-1} cm^{-2}, adjusted by the pixel scale difference between MUSE and S-PLUS), A_V and $\Sigma_\star$ maps. The color scales are matched to those of the same images in the Gao et al. (2021), who produced maps of these quantities derived on the basis of MUSE data over the inner $\sim 1 \times 1$ arcmin (marked by a box). The A_V map shown corresponds to the extinction applied to young stars and ELs.

4. Conclusions

After all, we conclude that the method using the code of spectral synthesis ALstar, recovers the stellar populations and emission line properties with good accuracy. We got really similar results to that one obtained by spectroscopy through simulation and also with real data. So, this means that the properties derived by S-PLUS data using the code ALstar are trustable and now we can apply the method in other galaxies.

Acknowledgements. Support from FAPESC and S-PLUS is duly acknowledged.

References

Bruzual G., Charlot S., 2003, MNRAS, 344, 1000
Calzetti D., Armus L., Bohlin R. C., Kinney A. L., Koornneef J., Storchi-Bergmann T., 2000, ApJ, 533, 682
Chabrier G., 2003, Publications of the Astronomical Society of the Pacific, 115, 763–795
Gao Y., Egusa F., Liu G., Kohno K., Bao M., Morokuma-Matsui K., Kong X., Chen X., 2021, ApJ, 913, 139
Iodice E., et al., 2019a, A&A, 623, A1
Iodice E., et al., 2019b, A&A, 627, A136
Mendes de Oliveira C., et al., 2019, MNRAS, 489, 241
Raj M. A., et al., 2019, A&A, 628, A4
Thainá-Batista J., et al., 2023, MNRAS, 526, 1874
Taylor E. N., et al., 2011, MNRAS, 418, 1587
Venturi G., et al., 2018, A&A, 619, A74
Werle A., Cid Fernandes R., Vale Asari N., Bruzual G., Charlot S., Gonzalez Delgado R., Herpich F. R., 2019, MNRAS, 483, 2382